Science of the Total Environment 764 (2021) 144275

Contents lists available at ScienceDirect

Science of the Total Environment

journal homepage: www.elsevier.com/locate/scitotenv

Spatiotemporal patterns and spatial risk factors for visceral leishmaniasis from 2007 to 2017 in Western and Central China: A modelling analysis

Dong Jiang [a,b,1], Tian Ma [a,b,1], Mengmeng Hao [a,b], Yushu Qian [a], Shuai Chen [a,b], Ze Meng [a], Liping Wang [c], Canjun Zheng [c], Xiao Qi [c,*], Qian Wang [a,b,**], Fangyu Ding [a,b,**]

[a] State Key Laboratory of Resources and Environmental Information System, Institute of Geographical Sciences and Natural Resources Research, Chinese Academy of Sciences, Beijing 100101, China
[b] College of Resources and Environment, University of Chinese Academy of Sciences, Beijing 100049, China
[c] National Institute for Viral Disease Control and Prevention, Chinese Center for Disease Control and Prevention (China CDC), Beijing 102206, China

HIGHLIGHTS

- The spatiotemporal patterns of VL cases in Western and Central China was analyzed.
- The relationships between VL and spatial risk factors were explored.
- Elevation has the most contribution to spatial heterogeneity of VL.
- The predicted risk zones of VL are mainly distributed in Western and Central China.

GRAPHICAL ABSTRACT

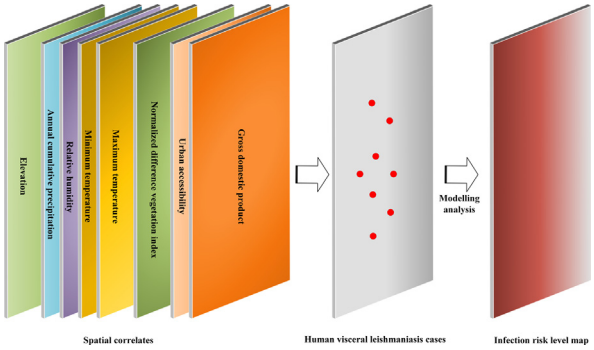

ARTICLE INFO

Article history:
Received 23 September 2020
Received in revised form 27 November 2020
Accepted 29 November 2020
Available online 25 December 2020

Editor: SCOTT SHERIDAN

Keywords:
Visceral leishmaniasis
Neglected diseases
Spatial risk factors
Spatiotemporal patterns
Public health

ABSTRACT

Visceral leishmaniasis (VL) is a neglected disease caused by trypanosomatid protozoa in the genus *Leishmania*, which is transmitted by phlebotomine sandflies. Although this vector-borne disease has been eliminated in several regions of China during the last century, the reported human VL cases have rebounded in Western and Central China in recent decades. However, understanding of the spatial epidemiology of the disease remains vague, as the spatial risk factors driving the spatial heterogeneity of VL. In this study, we analyzed the spatiotemporal patterns of annual human VL cases in Western and Central China from 2007 to 2017. Based on the related spatial maps, the boosted regression tree (BRT) model was adopted to explore the relationships between VL and spatial correlates as well as predicting both the existing and potential infection risk zones of VL in Western and Central China. The mined links reveal that elevation, minimum temperature, relative humidity, and annual accumulated precipitation make great contributions to the spatial heterogeneity of VL. The maps show that Xinjiang Uygur Autonomous Region, Gansu, western Inner Mongolia Autonomous Region, and Sichuan are predicted to fall in the highest infection risk zones of VL. Approximately 61.60 million resident populations lived in the high-risk regions of VL in Western and Central China. Our results provide a better understanding of how spatial risk factors driving VL spread as well as identifying the potential endemic risk region of VL, thereby enhancing the biosurveillance capacity of public health authorities.

* Corresponding author.
** Corresponding authors at: State Key Laboratory of Resources and Environmental Information System, Institute of Geographical Sciences and Natural Resources Research, Chinese Academy of Sciences, Beijing 100101, China.
E-mail addresses: qixiao@chinacdc.cn (X. Qi), wangq.17s@igsnrr.ac.cn (Q. Wang), dingfy.17b@igsnrr.ac.cn (F. Ding).
[1] These authors contributed equally to this work.

https://doi.org/10.1016/j.scitotenv.2020.144275

1. Introduction

Visceral leishmaniasis (VL), also known as kala-azar, is not only a life-threatening parasitic infection but also a largely zoonotic disease. It is caused by trypanosomatid protozoa in the genus *Leishmania* and is transmitted by phlebotomine sandflies (Lun et al., 2015; Pearson and Sousa, 1996). When the sandfly carrying the parasite bites human skin, *Leishmania* promastigotes are hypodermically injected and mostly ingested by macrophages (Braga et al., 2013). Promastigotes are transformed into amastigotes and then disseminated through the entire reticuloendothelial system via the vascular and lymphatic system, eventually resulting in their proliferation in bone marrow, liver, and spleen (Chappuis et al., 2007). Patients with VL typically presents several clinical manifestations including fever, hepatosplenomegaly, pancytopenia, pallor, cough, and abdominal distension (Fu et al., 2013; Wang et al., 2016; Zou et al., 2017). It will kill most patients within 2 years if untreated or appropriate treatment is not given, which is even faster than Acquired Immunodeficiency Syndrome (Kumar et al., 2014). Visceral leishmaniasis is widely distributed throughout America, Asia, Africa, and Europe and is endemic in up to 66 countries, which is associated with approximately 0.5 million new cases and 0.2–0.4 million deaths per year worldwide(Alvar et al., 2012; Desjeux, 2004; Murray et al., 2005; WHO, 2010). Based on the mortality and morbidity, World Health Organization (WHO) ranked this disease ninth in a global analysis of infectious diseases (WHO, 2010).

In China, the history of the struggle between people and VL can be traced back to the Qing Dynasty in 1904, which is nearly 120 years ago (Wang and Wu, 1959). Due to the lack of preventive measures and continuation of several wars, VL had become one of the most serious parasitic diseases that endanger people in China during the subsequent period from 1905 to 1950 (Cochran, 1914; Wang and Wu, 1959). In the 1950s, VL was once prevalent in the vast rural areas north of the Yangtze River involving 16 provinces and autonomous regions (Wang, 1985; Young, 1923). According to a detailed survey conducted by the government in 1951, there were about 530,000 VL cases in that year and the incidence rate in each county ranged from 10/100,000 to 500/100,000 (Geng, 1996; Wang et al., 2000a, 2000b). At that time, a comprehensive prevention and control measure designed by the government of the People's Republic of China was carried out stringently at every administrative level, which resulted in very remarkable results in the reduction of VL cases in the next decades (Fu et al., 2013; Guan and Shen, 1991; Wang, 1985; Xu, 1989). For instance, with this measure, VL in the North China Plain and the Shaanxi Guanzhong Plain had been basically under control by 1958, and by 1983, prevention of the disease in the entire plain of China had reached the elimination standard (Wang et al., 2000a, 2000b). However, since the late 1980s, the grand western development program implemented by the state provided a suitable habitat as a buffer for the spread of VL, which caused the recurrence and epidemic of VL in Western and Central China (Li et al., 2011). In the 1990s, VL was reported resurgent in 43 epidemic counties of 6 provinces in Western and Central China, including Xinjiang Uygur Autonomous Region, Gansu, Sichuan, Shaanxi, Shanxi, and Inner Mongolia Autonomous Region (Guan et al., 2000). Since 2000, VL has spread across more than 80 epidemic counties in 8 provinces (Han et al., 2019).

In recent decades, the incidence of VL has rebounded in several regions with the expansion of human activities and the enhancement of frequency, revealing that the disease remains a serious public health problem in Western and Central China (Ding et al., 2019; Li and Zheng, 2019; Wang et al., 2012; Zhou et al., 2020). However, the spatial epidemiological characteristics of VL in Western and Central China are still unclear, as the factors driving the spatial heterogeneity of VL. Based on the assembled data sets of annual VL cases and maps of spatial correlates, we were able to analyze the spatiotemporal dynamic patterns of VL cases in Western and Central China from 2007 to 2017, to explore the complex relationships between spatial correlates and VL, to map the potential infection risk zones of VL and to estimate the burden on public health imposed by the disease. By identifying the spatiotemporal patterns and generating the final predicted infection risk maps, this study is supposed to provide epidemiologists and local governments with significant information for prevention measures and control strategies.

2. Material and methods

The research area of this study contains 11 provinces in the western and central regions of China including Inner Mongolia, Qinghai, Ningxia, Gansu, Shaanxi, Shanxi, Xinjiang, Henan, Hubei, Chongqing, and Sichuan. We spatially match the clinical diagnosis and laboratory-confirmed VL cases (3682) with multi-dimensional spatial correlates including geographic, ecological, climatic, and socio-economic factors on the county level, and then construct the transmission risk model of VL using the machine learning algorithm. A boosted regression tree model (BRT) was adopted in this study to analyze the factors driving the spatial heterogeneity of VL and to generate potential transmission risk maps of VL in western and central China. Three types of key data sets are usually needed when building a BRT model: 1) a comprehensive data set of VL cases with detailed geographic information; 2) a set of spatial environmental and socioeconomic factors associated with VL, as shown in Table 1. 3) pseudo-absence records. In this study, all data were transformed into the same geographical coordinate system (WGS-84) and the same projected coordinate system (Albers Conical Equal Area).

2.1. Spatial correlates

2.1.1. Terrain factor

Terrain, though remains unclarified in the internal driving mechanism between itself and vector-borne diseases, has been affecting VL distribution for its great influence on both landscape and temperature. For example, it may, to a certain extent, have an indirect impact on the incubation and survival period of sand flies as well as its distribution as the hosts of parasites. There are some studies that have already explored the effect of elevation on the distribution of VL (Gao et al., 2017). And in this study, elevation was selected to be a potential terrain variable for VL presence. The elevation dataset with 90 m spatial resolution generated by the SRTM was downloaded from the CGIAR Consortium for Spatial Information (http://srtm.csi.cgiar .org, Access date: March 1, 2020). In addition, ArcGIS 10.2 and python 3.7 were employed to transform the elevation dataset from grid-level to the county-level.

Table 1
Spatial correlates adopted in this study.

Factor	Parameters	Data sources
Terrain	Elevation	Shuttle Radar Topography Mission (SRTM)
Ecological	NDVI	Global Inventory Modelling and Mapping Studies (GIMMS) group
Climatic	Annual cumulative precipitation	China Meteorological Data Service Centre (CMDC)
	Minimum temperature	
	Maximum temperature	
	Relative humidity	
Socioeconomic	Urban accessibility	European Commission Joint Research Centre (ECJRC)
	GDP	Global Change Research Data Publishing & Repository

Abbreviations: GDP, gross domestic product; NDVI, normalized difference vegetation index.

2.1.2. Ecological factor

Strong relationships between sand flies population presence and landscape have been reported in previous studies (Kuo et al., 2011; Quintana et al., 2014). For VL, vegetation plays an important role in the habitat for sand flies to survive by providing necessary resources and maintaining the water quality required by sand flies (Feliciangeli, 2004; Ready, 2013). In addition, previous studies have illustrated that spatial heterogeneity of VL is associated with land cover (WHO, 2010). For instance, the incidence of VL is often highest among people living at the edge of natural foci, i.e. forests and deserts. And some studies have found that the distribution of VL was relatively high in grassland and shrubland areas (Gao et al., 2017). In this study, NDVI was imported as a potential indicator to reflect the vegetation coverage intensity. We obtained the NDVI data with a spatial resolution of 8 × 8 km spanned 2007 to 2015 from the Global Inventory Modelling and Mapping Studies (GIMMS) group (https://ecocast.arc.nasa.gov/, Access date: March 10, 2020). The same way is implemented to convert the gridded NDVI data into the county-level.

2.1.3. Climatic factors

Climatic conditions are essential constraints on the transmission of vector-borne diseases (Olson and Scheer, 1978; Traub and Wisseman, 1974). Some previous studies have discovered that temperature, precipitation, and humidity have strong impacts on the survival, population, and distribution of sand flies and reservoir hosts (Hamta et al., 2020; Shirzadi et al., 2020). For instance, it is noted that precipitation and humidity have been proved to influence the reproduction and dormancy of vectors (Malaviya et al., 2011). Some other studies have also illustrated that temperature, precipitation, and humidity are related to the occurrence and distribution of VL (Gao et al., 2017; Li and Zheng, 2019). For example, Li et al. had found that increasing temperature or decreasing humidity could lead to incremental VL events (Li and Zheng, 2019), temperature, precipitation, and relative humidity are thusly taken as important climatic correlates in this study. Based on data obtained from China Meteorological Data Service Centre (http://data.cma.cn, Access date: March 10, 2020) of daily scale monitoring stations, the gridded datasets of monthly meteorological series with a spatial resolution of 1 km ranged from 2007 to 2017 was generated by ANUSPLIN-SPLINA software. In addition, a distribution map of meteorological factors including maximum temperature, minimum temperature, annual accumulated precipitation, and relative humidity at the county-level were generated based on ArcGIS 10.2 and python 3.7.

2.1.4. Socioeconomic factors

Previous studies have illustrated that socio-economic factors link to vector-borne diseases closely (Hasker et al., 2012; Wu et al., 2016). For instance, low-income people are more likely to be infected with VL for two reasons, one is the reduction of immunity caused by malnutrition, the other is poor housing conditions leading to the increasing reproduction and resting place of sand flies (Boelaert et al., 2009; Marcos-Marcos et al., 2018; WHO, 2010). Since the result of GDP is commonly used to measure the level of urbanization, we selected GDP data with a spatial resolution of 1 × 1 km in this study as one of the spatial drivers, which can be downloaded from the global change research data publishing & repository (http://www.geodoi.ac.cn, Access date: March 20, 2020). In addition, urbanization trends and human movement are taken as examples of key drivers in the expansion and transmission of vector-borne diseases (Aung et al., 2014; Ericsson et al., 2004). For example, the entry of a non-immune person into an epidemic area with existing vector-borne diseases may lead to new infection cases. On the other hand, liberalization of cross-regional trade may affect agricultural practices, which in turn may influence vectors and rodent hosts by changing the ecological landscape (Kuo et al., 2012). In the present study, we use the urban accessibility data with 1 × 1 km spatial resolution as a spatial driver that can be obtained free through the European Commission Joint Research Centre (ECJRC) (http://forobs.jrc.ec.europa.eu/, Access date: March 20, 2020). The socio-economic factors are converted to the county-level as well.

2.2. Occurrence and pseudo-absence records

In the present study, western and central China includes Inner Mongolia, Qinghai, Ningxia, Gansu, Shaanxi, Shanxi, Xinjiang, Henan, Hubei, Chongqing, and Sichuan. The known clinically-diagnosed and laboratory-confirmed VL human cases in western and central China from 2007 to 2017 were obtained from the Chinese Centre for Disease Control and Prevention (CDC) (http://www.chinacdc.cn/, Access date: March 1, 2020). Based on VL cases data with detailed information on the geographical locality, VL prevalence at county-level was obtained. In addition, each county with an average VL prevalence of greater than or equal to 1 person is regarded as high-risk samples, which is equivalent to occurrence records. While each county with no VL prevalence from 2007 to 2017 is regarded as low-risk samples, which also means pseudo-absence records. In total 231 occurrence records were dig out, and the same number of pseudo-absence records from low-risk areas were randomly selected correspondingly.

2.3. Modelling analysis

In the present study, a boosted regression model is employed to predict the potential transmission risk of VL based on 2007–2017 VL cases as well as multiple county-level environmental and socioeconomic predictors. Its functional form can be described as below:

$$f_t(X) = f_{t-1}(X) + \lambda \cdot \rho_t h(X; a_t) \quad \lambda \in (0, 1] \tag{1}$$

$$L(y, f(X)) = \log(1 + \exp(-2yf(X))) \tag{2}$$

$X = \{x_1, x_2, \cdots, x_n\}$ refers to related spatial environmental and socioeconomic correlates. y refers to VL risk. $f_t(X)$ represents the mapping function between X and y estimated at the t-th iteration. λ means learning rate. ρ_t means weight parameter. a_t defines segment variables. $h(X; a_t)$ links to the expression function of a single tree. ρ_t and a_t were generated by minimum loss function (Eq. (2)). More detailed information about BRT can be found somewhere else (Friedman, 2001; Ridgeway, 2006).

Based on occurrence and pseudo-absence records, a total sample (462) of VL will be constructed after each random selection process, and it will be randomly divided into training samples (75%; 348) and test samples (25%; 114). Based on these steps, version 3.3.3 of R statistical program was used to build BRT model combined with extended package "gbm" and "dismo". According to Messina's (Messina et al., 2016), the main adjustment parameters are set as follows: tree.complexity = 4, learning.rate = 0.005, bag.fraction = 0.75, step.size = 10, cv. folders = 10, max.trees = 10,000 while keep other parameters as default. Besides, we integrated an ensemble of 300 BRT models to increase the robustness of the fitted model and to quantify its uncertainty. In the process of fitting the model, a ten-fold cross-validation method is used to prevent overfitting, and the area under the curve (AUC) statistical indicator is applied to evaluate the accuracy of the ensemble models. Relative contribution (RC) index was used to estimate the relative importance of each spatial predictor during the modelling process.

3. Results

3.1. Spatiotemporal patterns

Fig. 1 reveals the spatial patterns of annual clinical and laboratory-confirmed human cases of VL reported from 2007 to 2017 in Western and Central China. In 2007, the reported human VL cases were mainly concentrated in the southeast part of Gansu, the central and southwest regions of Xinjiang Uygur Autonomous Region, and the northeast zone

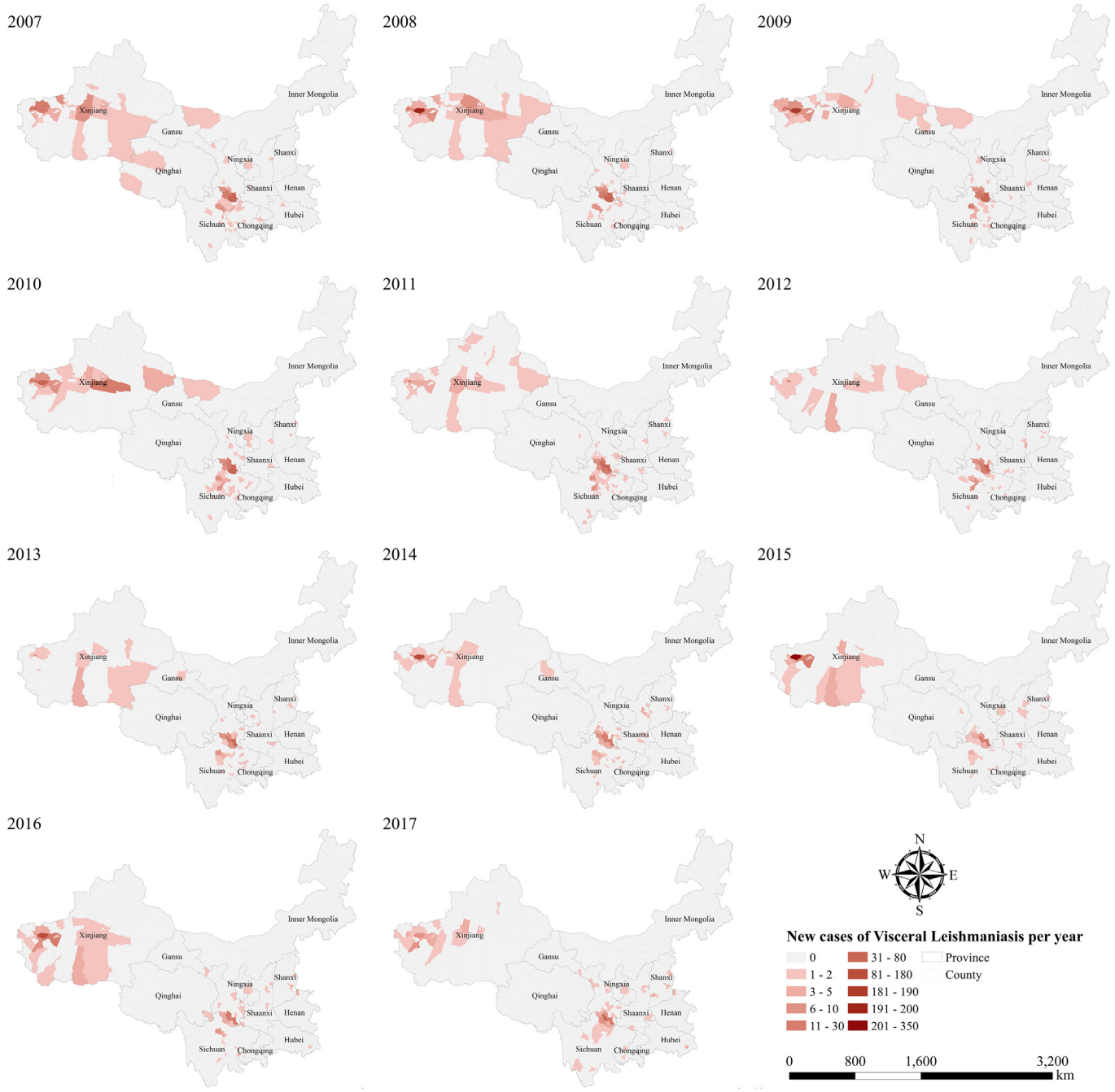

Fig. 1. Annual human cases of visceral leishmaniasis in Western and Central China from 2007 to 2017.

of Sichuan. For instance, Gansu ranks first (158 cases), followed by Xinjiang Uygur Autonomous Region (117 cases) and Sichuan (71 cases). The remaining new cases of VL in Western and Central China were scattered in Inner Mongolia Autonomous Region (2 cases), Shaanxi (2 cases), Chongqing (2 cases), Hubei (1 case), and Qinghai (1 case). In 2008, the number of new cases of VL in Xinjiang Uygur Autonomous Region increased significantly, reaching 300 cases, mainly distributed in the Kashgar region. Compared with cases in 2007 the number of new cases in Gansu decreased by 6, though its spatial distribution expanded slightly. Meantime, the number of new cases in Sichuan has decreased with its spatial distribution shrinking as well. From 2009 to 2011, new VL cases were still mainly distributed in Gansu, Xinjiang Uygur Autonomous Region, and Sichuan. During this period, the annual new cases in Gansu (153, 151, and 161 cases respectively) and Sichuan (58, 54, and 55 cases respectively) were relatively stable while the number of cases of VL in Xinjiang Uygur Autonomous Region has changed most with the number of new cases dropping from 289 to 57. Since 2011, the change in the number of new cases of VL in Xinjiang Uygur Autonomous Region has been fluctuating. For example, the number of new cases decreased from 41 to 26 during the period from 2012 to 2013, while it increased dramatically to 396 during the period from 2013 to 2015. In addition, the number of new cases in Xinjiang Uygur Autonomous Region decreased rapidly to 44 from 2015 to 2017. During the period from 2011 to 2017, the change in the number of new cases of VL in Gansu is relatively consistent with that in Sichuan. For instance, the number of new cases decreased to 53 (Gansu) and 15 (Sichuan) respectively during the period from 2011 to 2015, while the number of new cases increased to 95

(Gansu) and 27 (Sichuan) respectively during the period from 2015 to 2017. The annual new cases of VL in Shanxi and Shaanxi increased from 0 and 2 cases to 21 and 16 cases respectively during the period from 2007 to 2017 while the spatial distribution of the annual new cases in Shanxi was gradually expanding. Overall, the new cases of VL from 2007 to 2017 were mainly distributed in Xinjiang Uygur Autonomous Region, Gansu, and Sichuan of Western and Central China with a few cases scattering in other provinces. It should be noted that the number of new VL cases in the four provinces of Gansu, Sichuan, Shanxi, and Shaanxi is showing an increasing trend.

3.2. Relative contribution of spatial risk factors

Fig. 2 shows that elevation is the most important predictor in the ensemble BRT models, which is strongly correlated with the presence of VL, accounting for 31.52% (SE: 4.41%). Other main predictors including minimum temperature (positive correlation), relative humidity (positive correlation), annual accumulated precipitation (negative correlation), maximum temperature (complex association), NDVI (negative correlation) and urban accessibility (positive correlation) are accounting for12.75% (SE: 1.22%), 12.69% (SE: 2.95%), 11.22% (SE:3.29%), 9.83% (SE:2.62%), 9.30% (SE:3.07%) and 8.13% (SE: 2.63%) of variation explained by the ensemble BRT models respectively. In addition, it is shown that GDP (RC: 4.56%, SE: 1.81%, complex association) has little contribution to the ensemble BRT models.

3.3. Existing and potential infection risk zones

Validation statistics illustrated that the fitted ensemble BRT models obtained high predictive accuracy within Western and Central China with training dataset 10-fold cross-validation AUC = 0.833 ±0.025 and validation dataset AUC = 0.830 ± 0.041. Based on the mined relationship between the environmental predictors and the presence of the human VL cases, combined with the spatial environmental predictors at county level, we were able to predict the potential infection risk zones of VL in Western and Central China. Fig. 3 depicts the geographic distribution of the average infection risk level of VL in each county of Western and Central China which was generated from the ensemble BRT models. The predicted map reveals that Xinjiang Uygur Autonomous Region, Gansu, western Inner Mongolia Autonomous Region, and Sichuan are predicted to be the highest infection risk areas of VL. Meantime, the predicted infection risk of VL is also relatively high in the north-west regions of Qinghai, Chongqing City, Shaanxi, Hubei, and the western part of Henan.

We also estimated the predicted mean infection risk level map of VL throughout China (Supplementary Fig. 1) by combining the inferred patterns derived from the fitted BRT ensembles with county-scale related spatial correlates. The Supplementary Fig. 1A revealed that the predicted highest infection risk zones in unmodeled areas of China were mainly distributed in southeastern and western parts of Tibet Autonomous Region, central and northern regions of Yunnan, western and northern parts of Guizhou, western part of Hunan, and northern part of Guangxi Zhuang Autonomous Region. Based on upper and low bounds of the 95% confidence intervals of the fitted BRT ensembles, we also generated the predicted infection risk maps as shown in Supplementary Fig. 1B–1C. In addition, the uncertainty of the predicted risk level (Supplementary Fig. 1D) was quantified using standard deviation method, which illustrates a generally low level of the uncertainty of the fitted BRT ensemble.

3.4. Population at risk

To estimate the number of people located in the predicted infection risk zones, we adopted 0.5 as the threshold value and convert the continuous risk level map of VL into a binary map. Based on the county-level resident population distribution map in China derived from the Sixth National Census in 2010, we calculated the population living in the predicted VL infection risk zones within each province or municipality in Western and Central China, as shown in Table 2. Table 2 revealed that 61.60 million population in Western and Central China live in the predicted high infection risk areas of VL, with 95% confidence interval of 60.36–64.95 million. In Sichuan, the estimated population living in the predicted high infection risk areas is the largest among all the regions with about 29 million people, accounting for 46.67% of the total number of Western and Central China. The second is Chongqing (15.96%, 9.83 million people), followed by Gansu (12.36%, 7.61 million

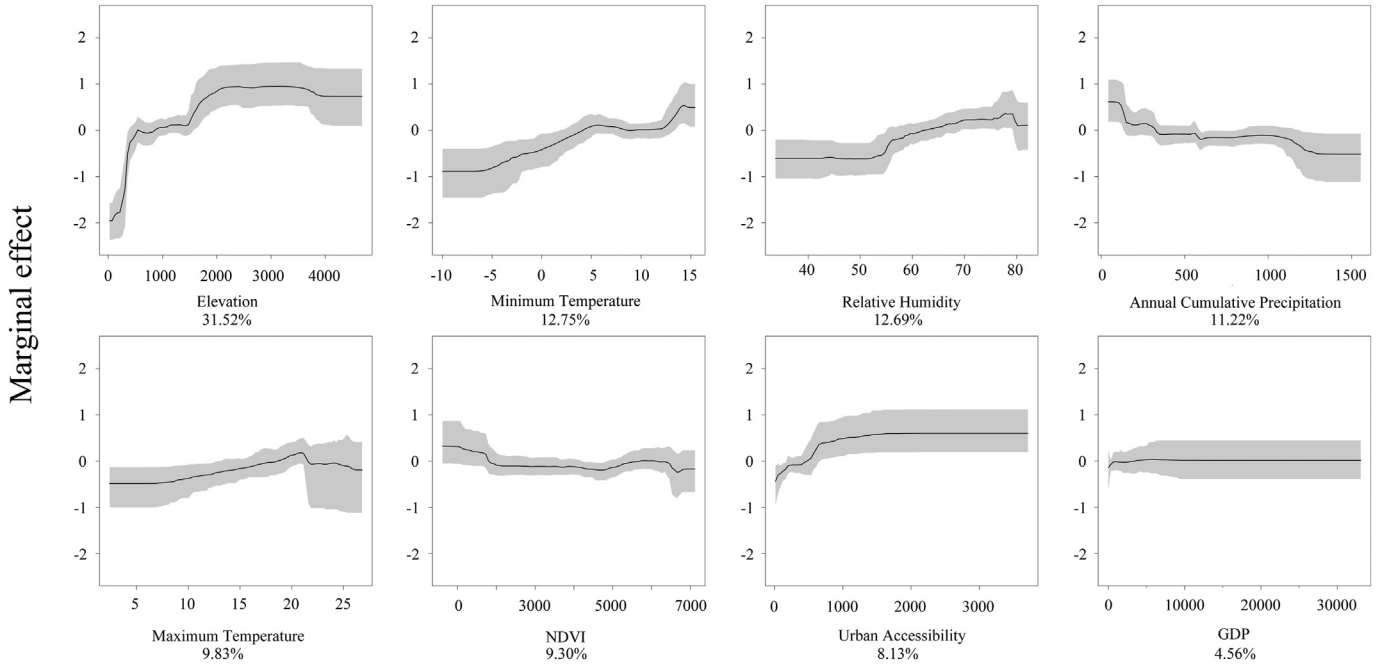

Fig. 2. Marginal effect curves of each predictor over the fitted BRT ensemble models. The black lines represent the mean effect curves, calculated from the ensemble BRT models. The shaded areas depict the predicted relationships to each predictor from all 300 BRT ensembles, within the 95% confidence interval.

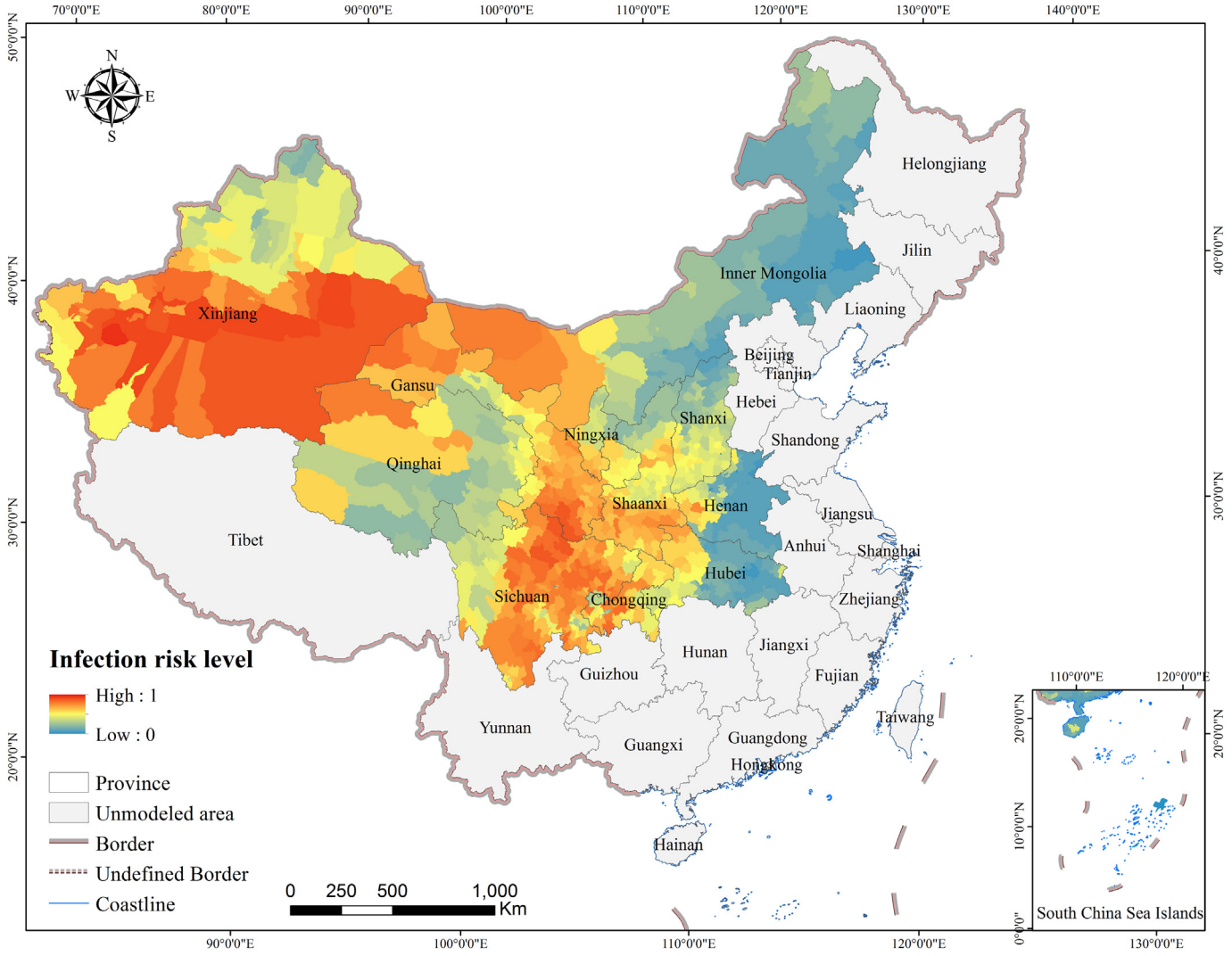

Fig. 3. Geographic distribution of infection risk level for VL in Western and Central China, with the risk level ranging from 0 (blue) to 1 (red).

people), Shaanxi (10.21%, 6.29 million people), Xinjiang Uygur Autonomous Region (6.02%, 3.71 million people), Hubei (3.51%, 2.16 million people) and Henan (2.34%, 1.44 million people). The estimated population living in high-risk areas of VL of the rest province (Shanxi, Ningxia, Qinghai, and Inner Mongolia) are all less than 1 million, with a total population of about 1.81 million people, accounting for nearly 1.83% of the total number.

Based on Supplementary Fig. 1, we further estimated approximately 34.35 million (ranges from 30.19 to 38.47 million) resident populations living in the predicted infection high-risk zones of VL within each province or municipality in the unmodeled regions of China, as shown in Supplementary Table 1. Notably, 91.4% of these residents are living in Yunnan (43.90%), Guizhou (26.05%), Hunan (14.76%), and Fujian (6.69%).

Table 2
Resident populations living in the predicted infection risk zones of visceral leishmaniasis within each province or municipality in Western and Central China.

Region	Population living in the predicted infection risk zones (Millions)	
	Average	95% confidence
Sichuan	28.75	28.55–29.03
Chongqing	9.83	9.83–10.77
Gansu	7.61	7.33–8.13
Shaanxi	6.29	5.98–7.20
Xinjiang	3.71	3.63–3.74
Hubei	2.16	2.10–2.44
Henan	1.44	1.35–1.44
Shanxi	0.68	0.45–0.49
Ningxia	0.49	0.49–0.49
Qinghai	0.43	0.43–0.54
Inner Mongolia	0.21	0.21–0.21
Western and Central China	61.60	60.36–64.95

4. Discussion

Based on the comprehensive VL infection records, we analyzed the spatiotemporal distribution characteristics of human VL cases in Western and Central China from 2007 to 2017. The result shows that VL is a long-term epidemic in northeastern Sichuan, southeastern Gansu, and Kashgar district in Xinjiang Uygur Autonomous Region, while in other areas VL cases are only sporadically distributed. On this basis, we predicted the existing and potential infection risk areas of the disease by combining VL cases and a set of county-scale spatial covariate layers in BRT models, illustrating that southern Xinjiang Uygur Autonomous Region, northern and southern Gansu, central and eastern Sichuan, central Chongqing, southern Tibet, and northern Yunnan are predicted to be high-risk areas for VL infection, which could be used

to form the design of detailed prevention and control strategies for VL in China.

During the period from 2007 to 2017, the annual human VL cases had been increasing in several provinces (i.e., Sichuan and Shanxi) as VL began to re-emerge, which accentuated the need to better understand the spatial risk factors driving the disease spread. In the present study, the complex relationships between VL and related spatial risk factors were explored based on the BRT modelling framework. For instance, elevation was estimated to be the most important predictor contributing to the occurrence of VL, which was consistent with some previous studies (Salahi-Moghaddam et al., 2010; Elnaiem et al., 2003). Our findings revealed that there was a significant positive correlation between elevation and VL occurrence, which may be due to the effect on the habitat (i.e., grassland and scrubland) distribution of disease vectors or rodent hosts (Gao and Zheng, 2019) of the increase in altitude. Besides, the marginal effect curves illustrated that climate factors have a profound effect on VL incidence. For instance, an increase in the spread risk of VL was observed as minimum temperature and maximum temperature initially increased, while a negative effect on the response was observed at a higher temperature. This pattern inferred from the modelling may be due to the mortality of adult sandflies when the temperature reaches a certain threshold temperature (Kasap and Alten, 2006). We also found that the spread risk of VL is positively correlated with relative humidity, which is consistent with some studies on the suitable habitat conditions that immature sand flies are usually more inclined to occupy cool and moist habitats (Ready et al., 1985; Ready, 2008). Overall, our findings are expected to have important implications, particularly in vector control strategies and management of risk associated with VL.

Compared with previous work on clinical manifestations, diagnosis and treatment, immunological characteristics, epidemiological characteristics (Leng, 1982; Yuan et al., 2017), a novel insight was provided to understand VL in Western and Central China from the perspective of space epidemiology. However, it is also important to realize that the probability of being exposed to the infection risk of VL varies with people due to their diversified occupation, behavioral habits as well as protective measures. For instance, it is shown that children under 5 years old are the main infected population because those children are under inadequate protection with little immunity (Zhao et al., 2015; Zheng et al., 2017). In future work, we will make efforts in collecting comprehensive and detailed population-related data to accurately assess the health burden imposed by VL on China.

CRediT authorship contribution statement

Dong Jiang: Methodology, Software, Resources, Data curation, Writing – original draft, Funding acquisition. **Tian Ma:** Methodology, Software, Formal analysis, Data curation, Writing – original draft, Visualization. **Mengmeng Hao:** Investigation, Resources, Data curation. **Yushu Qian:** Investigation, Resources, Data curation. **Shuai Chen:** Investigation, Resources, Data curation. **Ze Meng:** Investigation, Resources, Data curation. **Liping Wang:** Investigation, Resources, Data curation. **Canjun Zheng:** Investigation, Resources, Data curation. **Xiao Qi:** Conceptualization, Supervision, Writing – review & editing, Project administration. **Qian Wang:** Conceptualization, Methodology, Data curation, Writing – original draft, Supervision. **Fangyu Ding:** Conceptualization, Validation, Supervision, Writing – review & editing, Project administration.

Declaration of competing interest

The authors declare that they have no competing interests.

Acknowledgments

We thank Qiaoling Zhu for providing valuable suggestions and myriad research staff who participated in compiling the most comprehensive occurrence dataset of visceral leishmaniasis.

Availability of data and materials

All relevant data are contained within the manuscript.

Funding

This research is supported and funded by the Strategic Priority Research Program of the Chinese Academy of Sciences (XDA19040305) and the China Mega-Project on Infectious Disease Prevention (No. 2018ZX10713001).

Appendix A. Supplementary data

Supplementary data to this article can be found online at https://doi.org/10.1016/j.scitotenv.2020.144275.

References

Alvar, J., Velez, I.D., Bern, C., Herrero, M., Desjeux, P., Cano, J., et al., 2012. Leishmaniasis worldwide and global estimates of its incidence. PLoS One 7, e35671.
Aung, A.K., Spelman, D.W., Murray, R.J., Graves, S., 2014. Rickettsial infections in southeast asia: implications for local populace and febrile returned travelers. American Journal of Tropical Medicine & Hygiene 91, 451–460.
Boelaert, M., Meheus, F., Sanchez, A., Singh, S.P., Sundar, S., 2009. The poorest of the poor: A poverty appraisal of households affected by visceral leishmaniasis in Bihar, India. Tropical Med. Int. Health 14, 639–644.
Braga, A.S.C., Toledo Junior, A.C.C., Rabello, A., 2013. Factors of poor prognosis of visceral leishmaniasis among children under 12 years of age. Rev. Soc. Bras. Med. Trop. 46, 55–59.
Chappuis, F., Sundar, S., Hailu, A., Ghalib, H., Rijal, S., Peeling, R.W., et al., 2007. Visceral leishmaniasis: what are the needs for diagnosis, treatment and control? Nat. Rev. Microbiol. 5, 873.
Cochran, S., 1914. Distribution of kala-azar in China and Korea. China Med J 28, 274–276.
Desjeux, P., 2004. Leishmaniasis: current situation and new perspectives. Comp. Immunol. Microbiol. Infect. Dis. 27, 305–318.
Ding, F.Y., Wang, Q., Fu, J.Y., Chen, S., Hao, M.M., Ma, T., et al., 2019. Risk factors and predicted distribution of visceral leishmaniasis in the Xinjiang Uygur autonomous region, China, 2005–2015. Parasit. Vectors 12, 1–10.
Elnaiem, D.E.A., Schorscher, J., Bendall, A., Obsomer, V., Osman, M.E., Mekkawi, A.M., et al., 2003. Risk mapping of visceral leishmaniasis: the role of local variation in rainfall and altitude on the presence and incidence of kala-azar in eastern Sudan. The American journal of tropical medicine and hygiene 68 (1), 10–17.
Ericsson, C.D., Jensenius, M., Fournier, P.E., Raoult, D., 2004. Rickettsioses and the international traveler. Clinical Infectious Diseases 10.
Feliciangeli, M.D., 2004. Natural breeding places of phlebotomine sandflies. Medical & Veterinary Entomology 18, 71–80.
Friedman, J.H., 2001. Greedy function approximation: a gradient boosting machine. Ann. Stat. 29 (5), 1189–1232.
Fu, Q., Li, S.Z., Wu, W.P., Hou, Y.Y., Zhang, S., Feng, Y., et al., 2013. Endemic characteristics of infantile visceral leishmaniasis in the people's Republic of China. Parasit. Vectors 6, 143.
Gao, Xiang, Zheng, Cao, 2019. Meteorological conditions, elevation and land cover as predictors for the distribution analysis of visceral leishmaniasis in Sinkiang province. Mainland China, Science of The Total Environment 646, 1111–1116.
Gao, X., Qin, H.Y., Xiao, J.H., Wang, H.B., 2017. Meteorological conditions and land cover as predictors for the prevalence of bluetongue virus in the Inner Mongolia autonomous region of mainland China. Preventive Veterinary Medicine 138, 88–93.
Geng, G., 1996. Epidemiology. Vol. 2. People's Medical Publishing House, Beijing.
Guan, L.R., Shen, W.X., 1991. Recent advances in visceral leishmaniasis in China. The Southeast Asian journal of tropical medicine and public health 22, 291–298.
Guan, L.R., Qu, J.Q., Chai, J.J., 2000. Leishmaniasis in China present status of prevalence and some suggestions on its control. Endem Dis Bull China 15 (3), 49–52.
Hamta, A., Saghafipour, A., Farahani, L.Z., Asl, E.M., Ghorbani, E., 2020. The granger causality analysis of the impact of climatic factors on visceral leishmaniasis in northwestern Iran in 1995–2019. J. Parasit. Dis. 1–7.
Han, S., Wu, W.P., Xue, C.Z., Ding, W., Hou, Y.Y., Feng, Y., et al., 2019. Endemic status of visceral leishmaniasis in China from 2004 to 2016. Chin J Parasitol Parasit Dis 37 (2), 189–195.
Hasker, E., Singh, S.P., Malaviya, P., Picado, A., Gidwani, K., Singh, R.P., et al., 2012. Visceral leishmaniasis in rural Bihar, India. Emerg. Infect. Dis. 18, 1662–1664.
Kasap, O.E., Alten, B., 2006. Comparative demography of the sand fly phlebotomus papatasi (diptera: Psychodidae) at constant temperatures. Journal of Vector Ecology 31, 378–385.
Kumar, V.D., Verma, P.R., Singh, S.K., 2014. New insights into the diagnosis and chemotheraphy for visceral leishmaniasis. Curr Drug Deliv 11, 200–213.
Kuo CC, Huang JL, Ko CY, Lee PF, Wang HC. 2011. Spatial analysis of scrub typhus infection and its association with environmental and socioeconomic factors in Taiwan. Acta Trop. 120:0–58.
Kuo, C.C., Huang, J.L., Shu, P.Y., Lee, P.L., A. Kelt D, Wang HC., 2012. Cascading effect of economic globalization on human risks of scrub typhus and tick-borne rickettsial diseases. Ecol. Appl. 22, 1803–1816.

Leng, Y.J., 1982. A review of kala-azar in China from 1949 to 1959. Trans. R. Soc. Trop. Med. Hyg. 76, 531–537.
Li, Y., Zheng, C.J., 2019. Associations between meteorological factors and visceral leishmaniasis outbreaks in jiashi county, Xinjiang Uygur autonomous region, China, 2005–2015. Int. J. Environ. Res. Public Health 16, 1775.
Li, Y.F., Zhong, W.X., Zhao, G.H., Wang, H.F., 2011. Prevalence and control of kala-azar in China. J Pathog Biol 6, 629–631.
Lun, Z.R., Wu, M.S., Chen, Y.F., Wang, J.Y., Zhou, X.N., Liao, L.F., et al., 2015. Visceral leishmaniasis in China: an endemic disease under control. Clin. Microbiol. Rev. 28, 987–1004.
Malaviya, P., Picado, A., Singh, S.P., Hasker, E., Singh, R.P., Boelaert, M., Sundar, S., 2011. Visceral leishmaniasis in Muzaffarpur district, Bihar, India from 1990 to 2008. PloS one 6 (3), e14751. https://doi.org/10.1371/journal.pone.0014751.
Marcos-Marcos, J., de Labry-Lima, A.O., Toro-Cardenas, S., Lacasaña, M., Degroote, S., Ridde, V., et al., 2018. Impact, economic evaluation, and sustainability of integrated vector management in urban settings to prevent vector-borne diseases: a scoping review. Infectious Diseases of Poverty.
Messina, J.P., Kraemer, M.U.G., Brady, O.J., Pigott, D.M., Shearer, F.M., Weiss, D.J., Golding, N., Ruktanonchai, C.W., Gething, P.W., Cohn, E., Brownstein, J.S., Khan, K., Tatem, A.J., Jaenisch, T., Murray, C.J.L., Marinho, F., Scott, T.W., Hay, S.I., 2016. Mapping global environmental suitability for Zika virus. Elife 5, 1–19. https://doi.org/10.7554/eLife.15272.
Murray, H.W., Berman, J.D., Davies, C.R., Saravia, N.G., 2005. Advances in leishmaniasis. Lancet 366, 1561–1577.
Olson, J.G., Scheer, E.J., 1978. Correlation of scrub typhus incidence with temperature in the pescadores islands of Taiwan. Annals of Tropical Medicine & Parasitology 72, 195–196.
Pearson, R.D., Sousa, A.Q., 1996. Clinical spectrum of Leishmaniasis. Clin. Infect. Dis. 22, 1–13.
Quintana, M.G., Salomón, O.D., Lizarralde, D.G.M.S., 2014. Distribution of phlebotomine sand flies (diptera: Psychodidae) in a primary forest-crop interface, salta, argentina. Journal of Medical Entomology 6.
Ready, P.D., 2008. Leishmania manipulates sandfly feeding to enhance its transmission. Trends Parasitol. 24 (4), 151–153.
Ready, Paul D., 2013. Biology of phlebotomine sand flies as vectors of disease agents. Annu. Rev. Entomol. 58, 227–250.
Ready, P.D., Arias, J.R., Freitas, R.A., 1985. A pilot study to control lutzomyia umbratilis (diptera: Psychodidae) the major vector of leishmania braziliensis guyanensis, in a periurban rainforest of Manaus, Amazonas state, Brazil. Memorias do Instituto Oswaldo Cruz 80.
Ridgeway, G., 2006. Gbm: generalized boosted regression models. R package version 1 (3), 55.
Salahi-Moghaddam, A., Mohebali, M., Moshfae, A., Habibi, M., 2010. Ecological study and risk mapping of visceral leishmaniasis in an endemic area of Iran based on a geographical information systems approach. Geospat. Health 5 (1), 71–77.
Shirzadi, M.R., Javanbakht, M., Vatandoost, H., Jesri, N., Saghafipour, A., Fouladi-Fard, R., Omidi-Oskouei, A., 2020. Impact of environmental and climate factors on spatial distribution of cutaneous Leishmaniasis in northeastern Iran: utilizing remote sensing. J. Arthropod. Borne Dis. 14 (1), 56.
Traub, R., Wisseman, C.L., 1974. Review article: the ecology of chigger-borne rickettsiosis (scrub typhus). J. Med. Entomol. 11, 237–303.
Wang, C.T., 1985. Leishmaniasis in China: Epidemiology and Control Program. Leishmaniasis Elsevier Biomedical Press, Amsterdam, The Netherlands, pp. 469–478.
Wang, C.T., Wu, C.C., 1959. Kala-azar. People's Health Publisher, Beijing, China.
Wang, Z., Xiong, G., Guan, L., 2000a. Epidemiology and prevention of kala-azar in China. Chinese Journal of Epidemiology 21, 51.
Wang, Z.J., Xiong, G.H., Guan, L.R., 2000b. Achievement on the epidemiology and control of kala-azar in China. Chinese Journal of Epidemiology 21 (1), 51–54.
Wang, J.Y., Cui, G., Chen, H.T., Zhou, X.N., Gao, C.H., Yang, Y.T., 2012. Currentepidemiologicalprofileandfeatures of visceral leishmaniasis in people's Republic of China. Parasites Vectors 5, 1–11.
Wang, L.Y., Wu, W.P., Fu, Q., Guan, Y.Y., Han, S., Niu, Y.L., et al., 2016. Spatial analysis of visceral leishmaniasis in the oases of the plains of kashi prefecture, Xinjiang Uygur autonomous region, China. Parasit. Vectors 9, 1–7.
WHO, 2010. Control of the Leishmaniases: Report of a Meeting of the Who Expert Committee on the Control of Leishmaniases. World Health Organization.
Wu, Y.C., Qian, Q., Soares Magalhaes, R.J., Han, Z.H., Hu, W.B., Haque, U., et al., 2016. Spatiotemporal dynamics of scrub typhus transmission in mainland china, 2006-2014. PLoS Negl. Trop. Dis. 10.
Xu, Z.B., 1989. Present situation of visceral leishmaniasis in China. Parasitol. Today 5, 224–228.
Young, C.W., 1923. Kala-azar in china. China Medical Journal 37.
Yuan, D.M., Qin, H.X., Zhang, J.G., Liao, L., Chen, Q.W., Chen, D.L., et al., 2017. Phylogenetic analysis of hsp70 and cyt b gene sequences for chinese leishmania isolates and ultrastructural characteristics of chinese leishmania sp. Parasitol. Res. 116, 693–702.
Zhao, S., Li, Z., Zhou, S., Zheng, C., Ma, H., 2015. Epidemiological feature of visceral leishmaniasis in China, 2004-2012. Iran. J. Public Health 44, 51–59.
Zheng, C.J., Xue, C.Z., Wu, W.P., Zhou, X.N., 2017. Epidemiological characteristics of kala-azar disease in China, during 2005-2015. Zhonghua liu xing bing xue za zhi = Zhonghua liuxingbingxue zazhi 38, 431–434.
Zhou, Z.B., Wang, J.Y., Gao, C.H., Han, S., Li, Y.Y., Zhang, Y., et al., 2020. Contributions of the national institute of parasitic diseases to the control of visceral leishmaniasis in china. National Institute of Parasitic Diseases, China: 70 Years and Beyond, p. 185.
Zou, L., Chen, J., Ruan, S., 2017. Modeling and analyzing the transmission dynamics of visceral leishmaniasis. Mathematical Biosciences & Engineering 14, 1585–1604.